Langmuir

Article

pubs.acs.org/Langmuir

Encapsulation of Clay within Polymer Particles in a High-Solids Content Aqueous Dispersion

Yuri Reyes,[†] Pablo J. Peruzzo,[†] Mercedes Fernández,[‡] Maria Paulis,*[,†] and Jose R. Leiza*[,†]

[†]POLYMAT, Kimika Aplikatua Saila, Kimika Zientzien Fakultatea, University of the Basque Country UPV/EHU, Joxe Mari Korta Zentroa, Tolosa Hiribidea 72, 20018 Donostia-San Sebastián, Spain

[‡]POLYMAT, Polimeroen Zientzia eta Teknologia Saila, Kimika Zientzien Fakultatea, University of the Basque Country UPV/EHU, Joxe Mari Korta Zentroa, Tolosa Hiribidea 72, 20018 Donostia-San Sebastián, Spain

Supporting Information

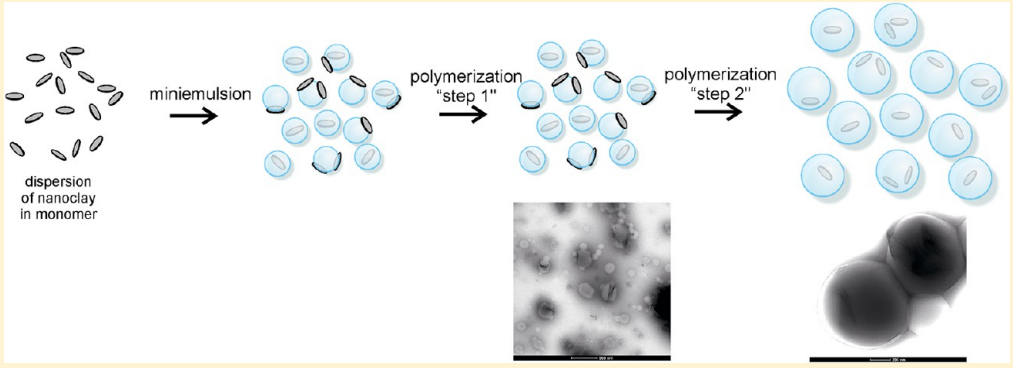

ABSTRACT: By using a two-step polymerization process, it was possible to encapsulate clay platelets within polymer particles dispersed in water. First, seed polymer particles with chemically bonded clay were obtained by batch miniemulsion polymerization. Then, the clay was buried within the particles by the addition of neat monomer in a second step. The final stable dispersions can have a solids content of up to 50 wt %. Transmission electron microscopy images clearly show the presence of clay platelets inside the polymer colloids, although they are not totally exfoliated. The obtained nanocomposites showed an increase in both the storage modulus in the rubbery state and the water resistance as the clay content increases. The approach presented here might be useful for encapsulating other high-aspect ratio nanofillers.

INTRODUCTION

The addition of layered fillers to polymer matrices is a very common technique used to improve the properties of polymeric materials. If the compatibility between the filler and the polymer is the correct one, the final properties might not only be a combination of the individual components, but a synergistic effect may be achieved. Otherwise, the properties can be damaged. Clay is a very common inorganic filler.[1,2] The addition of clay improves, for instance, the mechanical,[3] thermal,[4] adhesive,[5] and permeation[6,7] properties of polymers. To make the inorganic filler compatible with the polymer, the surface of the clay must be modified.[8] Moreover, if chemical bonds between the clay and the polymer are present, some properties may be substantially enhanced.[9]

With this idea in mind, plenty of work has been done to produce polymer composites dispersed in aqueous media, mainly using emulsion polymerization, in which inorganic fillers remain attached to the polymer particles.[1,10] However, because of the complexity of the emulsion polymerization mechanism (polymerization in the aqueous and organic phases, transport of the monomer from large droplets to the growing polymer particles, radical entry and exit, etc.), it is not so easy to have good control over the final particle structure; i.e., it is difficult to retain the layered filler within the latex particles, so the filler remains in the aqueous phase or at the surface of the polymer particles. Moreover, the presence of clay decreases the latex stability, lowering the maximal solids content of stable dispersions,[11] which hinders the large scale application of such hybrid materials. Better control of the particle structure can be achieved by miniemulsion polymerization.[12] In this technique, large monomer droplets are reduced in size from micrometers to hundreds of nanometers via application of a high shear. Once the miniemulsion is obtained, the monomer droplets should have the average composition of the original organic phase. In a miniemulsion polymerization, the polymerization is conducted mainly in the monomer droplets, and therefore, they become polymer particles.[13] That is why this technique is useful for the production of either organic−organic[14,15] or organic−inorganic[16−18] hybrid polymer particles with better control of particle structure.

Received: April 8, 2013
Revised: July 2, 2013
Published: July 8, 2013

Specifically, in the case of inorganic fillers, it is important that both components, the filler and the monomer system, are compatible enough; otherwise, the properties of the final material might not change or could be damaged. If the compatibility of the filler is tuned with the monomer system and with the aqueous phase, it is possible to place the filler on the surface or within the monomer droplet, either homogeneously distributed in the polymer particle or forming aggregates. However, for high-aspect ratio fillers, such as clays, carbon nanotubes, graphene flakes, rodlike nanoparticles, some pigments, etc., even if the inorganic material is rather compatible with the monomer system, the filler is preferentially located at the water−monomer interphase because of the entropic contribution; additionally, for the high-aspect ratio material to be encapsulated, the monomer droplet or polymer particle must be large enough to contain the filler.[19,20]

As a result, clay-armored or dumbbell-like latex particles are commonly obtained by different polymerization approaches[21,22] (including miniemulsion), and only few examples of true clay encapsulation are available, using rather complex procedures[23,24] and low-solids content dispersions.[25,26] In particular, the increase in the solids content is challenging if one wants to keep a percentage of clay that would enhance the performance of the final film. There are reports in the literature that show how difficult is to increase the solids content when the clay content is above a few percent because of the large amount of electrolytes that increase the ionic strength of the aqueous phase that jeopardize the stability of the polymer particles.[11,27] The development of a procedure for encapsulating clay, and other high-aspect ratio fillers, opens the opportunity to obtain new hybrid particles with a morphology not obtained until now, with a strong impact on the properties of these systems. Because of their unique morphology and improved interfacial properties, the films obtained from these structured nanocomposites can exhibit improved performance properties compared to conventional composites and may show different mechanical, rheological, and water uptake behavior depending on the clay location, dispersion, and load.[28,29] Contrary to previous approaches that use exclusively conventional emulsion or miniemulsion polymerization as an attempt to encapsulate clay, the approach presented here comprises the synthesis of the seed particles by batch miniemulsion polymerization to place and chemically attach the clay either within or on the surface of the polymer particles. Then, in a second step, neat monomer and initiator are added to bury the clay while the seed particles grow in size, allowing the synthesis of a stable dispersion with a solids content of 50 wt %. The final clay content is varied between 0.3 and 1.7 wt % with respect to the solids of the dispersion. To have a stable latex at such solids contents and polymer particles large enough to hold the clay, poly(vinyl alcohol) is used as protective colloid, instead of standard surfactants. The morphology of the particles and films was studied by transmission electron microscopy. X-ray diffraction was used to study the degree of exfoliation of the clay platelets. Thermal, water sorption, and viscoelastic properties of films obtained from the hybrid particles were also studied. It was demonstrated that the presence of clay encapsulated in the polymer particles produced an increase in T_g and in the storage modulus in the rubbery state without changes in the thermal stability, together with an improvement in the water resistance of these nanocomposite materials.

EXPERIMENTAL SECTION

Materials. Commercial natural clay (Cloisite Na) (provided by Southern Clay Products Inc., with a cationic exchange capacity of 92.6 mequiv/100 g of clay and a range of platelet sizes between 30 and 300 nm[30]) was organo-modified with 2-methacryloylethylhexadecyldimethylammonium bromide (MA16) (obtained via the synthetic procedure used by Zeng et al.[31]) to make it reactive in the free radical polymerization as shown elsewhere.[9] The monomer vinyl acetate (VAc) from Quimidroga was used as received. Poly(vinylalcohol)'s, PVA's, Mowiol 23−88, and Mowiol 28−99 were kindly provided by Kuraray. A mixture of Mowiol 23−88 and Mowiol 28−99 at a 3/1 weight ratio was used. Potassium persulfate (KPS) and sodium bicarbonate, both from Aldrich, were used as received.

Miniemulsion Preparation. The compositions of the miniemulsions prepared in this work are presented in step 1 of Table 1.

Table 1. Formulations Used in the Synthesis of the Hybrid Polymer Particles

substance	step 1 (g)	step 2 (g)	cooking (g)
monomer, VAc	56.45	136.05	–
modified Cloisite Na	variable (0.00, 0.65, 2.00, or 3.50)	–	–
buffer ($NaHCO_3$) at 2.44 wt %	14.00	–	–
initiator (KPS) at 1.6 wt %	28.55	13.80	2.25
PVA solution at 7.30 wt %	157.5	–	–

The modified clay (0.65, 2.00, or 3.50 g) was dispersed in the monomer (corresponding to the first step) by being ultrasonicated for 5 min and magnetically stirred overnight. The highest clay content of this dispersion (clay and monomer) was 6.2 wt %, where the clay might be forming a Wigner glass that generates a dispersion with high viscosity;[32] going to a higher clay content would substantially increase the viscosity of the dispersion, making it unmanageable. The PVA aqueous solution (obtained by dissolving the PVA at 90 °C for 2 h) and the buffer solution were mixed with the clay−monomer dispersion by being magnetically stirred for 15 min. This mixture was used to prepare a miniemulsion using ultrasound (Branson Sonifier 450, operating at 8-output control and 80% duty cycle for 5 min) together with magnetic stirring and an ice bath.

Polymerization. The polymerization was conducted in two steps using the formulation shown in Table 1. The miniemulsion was loaded in a 0.5 L glass reactor while being mechanically stirred under a nitrogen atmosphere. Once the system reached the desired temperature, 65 °C, the KPS initiator solution corresponding to the first step was fed over 5 min. This miniemulsion was left to react for 1 h. When the seed prepared by batch miniemulsion polymerization was obtained, the temperature was increased to 70 °C, and then the monomer and initiator solution corresponding to step 2 (see Table 1) were fed over 3 h. After the feeding period, a shot of the initiator solution (2.25 g) was added and the latex was left at 70 °C for 1 h before being cooled. A sample without clay was prepared for comparative purposes.

Characterization. Transmission electron microscopy (TEM) (Tecnai G2 Twin) was used to analyze the structure of the particles. The latexes, both the seed and the final form, were diluted (~0.1 wt %), and a drop was left to dry at 5 °C on the TEM grid. Also, films from the latexes were obtained in silicon molds at 23 °C and 55% relative humidity. Cross-sectional areas ~100 nm in thickness were obtained by (cryo)microtomy at −25 °C (Leica EM UC6). No staining agent was used in any of the samples. Wide-angle X-ray diffraction (WAXD) analyses were performed on a Philips PW 1729 generator connected to a PW 1820 instrument (Cu KR radiation with wavelength λ = 0.154056 nm) at room temperature. The dynamic viscoelastic behavior of samples was investigated using a stress-controlled rotational rheometer (ARG2, TA Instruments) with

dx.doi.org/10.1021/la401301s | Langmuir 2013, 29, 9849−9856

parallel-plate geometry (12 mm diameter). Specimens 12 mm in diameter and 1 mm in thickness were prepared and dried at ~20 °C. Temperature sweep experiments in the linear regime were conducted under a nitrogen atmosphere at 1 Hz; the cooling rate was 2 °C/min, and the temperature was varied from 150 to 60 °C. Prior to the measurement, the linear viscoelastic conditions were established by a torque sweep test, and all tests were conducted under 0.1% deformation and 4 N normal force. Differential scanning calorimetry (DSC) was performed using a Shimadzu DSC-60 instrument, between −50 and 240 °C, at a heating rate of 10 °C/min. Samples were first heated to 100 °C at a rate of 30 °C/min and cooled at a rate of 30 °C/min before being scanned to erase the thermal history. A nitrogen gas purge was applied, and the second heating curves were used for analysis. Thermogravimetric analysis (TGA) was obtained using a TA Instruments thermogravimetric analyzer (model Q500) from 20 to 700 °C with a heating rate of 10 °C/min under a nitrogen atmosphere; to degrade the organic components, air was injected at 700 °C for 5 min. For the water uptake measurements, specimens 20 mm in diameter and 1 mm in thickness were prepared and dried at 20 °C. They were immersed in distilled water at room temperature. Specimens were periodically removed from water, dried with filter paper, and immediately weighed with a precision of 0.01 mg before being returned to the water bath. The relative mass uptake was determined using eq 1:

$$\mathrm{Mt}\,(\%) = \left(\frac{W_t - W_0}{W_0}\right) \times 100 \qquad (1)$$

where W_t and W_0 are the instantaneous and initial weights, respectively.

RESULTS AND DISCUSSION

Morphology of the Nanocomposites. The presence of methacrylic groups on the clay surface that would react during free radical polymerization was confirmed by Fourier transform infrared and ^{1}H nuclear magnetic resonance methods. From TGA measurements, the organic content of the modified clay is 32 wt % (see the Supporting Information).

The localization of this clay in the synthesized polymer colloids was studied by TEM as discussed below. Figure 1

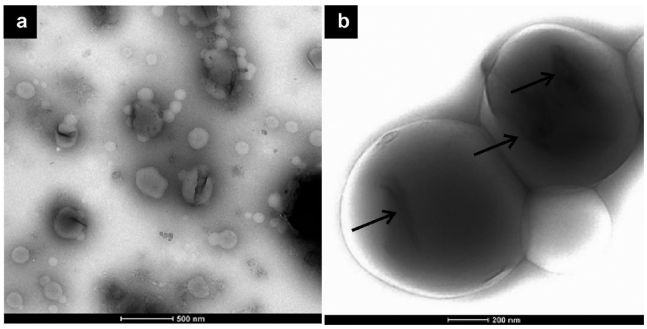

Figure 1. TEM image of individual particles of (a) the seed polymer particles obtained by miniemulsion and (b) the final latex of the sample containing 1.0 wt % clay (the contrast was enhanced to better visualize the interior of the particles). The dark lines correspond to the clay, indicated by black arrows.

shows TEM images of individual hybrid particles of the seed and final latex for the sample containing 1.0 wt % clay. In the seed particles (Figure 1a), it can be seen that the clay platelets are placed either within or on the surface of the polymer particles; furthermore, in some polymer particles, mainly the small ones, there is no clay at all, although its presence cannot be ruled out because the encapsulation of nanometric fragments of clay in polymer particles has been reported.[33] However, it is worth noting that mild sonication conditions were used in this work, and hence, fragmentation of the clay platelet is not likely; therefore, the platelets should be seen if they are present in the small particles of the seed. The particle size distribution is rather broad (see the Supporting Information), which is common in systems that use poly(vinyl alcohol) as a protective colloid instead of standard surfactants.[34] On the other hand, in the final latex particles, the clay is not easily observed because the particles are rather large and the electron beam is not able to cross through the particles, so they appear very dark.[35] However, in many particles, some dark lines corresponding to the clay are observed (see the additional TEM images in the Supporting Information).

To better visualize the location of the clay and avoid any misleading interpretation,[36,37] TEM images of thin cross sections of the films were obtained and are shown in Figure 2 for the sample with 1.0 wt % clay. The polymer particles in

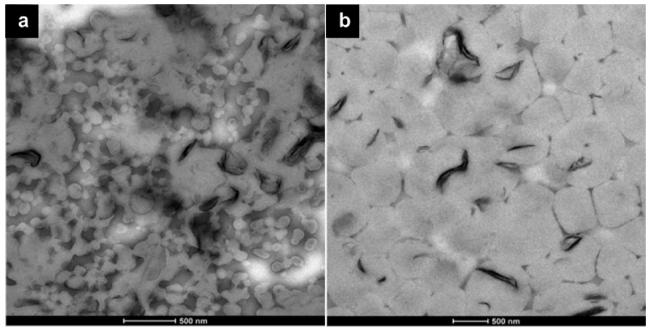

Figure 2. TEM image of thin cross-sectional portions of the films corresponding to (a) the seed obtained by miniemulsion polymerization and (b) the final latex for the sample containing 1.0 wt % clay.

the film retain more or less the spherical shape because of limited particle deformation and chain interdiffusion between neighboring particles, because the film was formed at a temperature (23 °C) lower than the glass transition temperature of the polymers[38] (~28 °C for PVAc[39] and ~58 and ~85 °C for PVA, depending on the degree of hydrolysis[40]). The TEM image of the film obtained from the seed particles (Figure 2a) clearly shows the broadness of the particle size distribution (See also the Supporting Information). The spaces between the PVAc particles are filled with PVA (note that 16.9 wt % of the seed polymer is PVA). The brightest domains are caused by the rupture of the film during the cut. In the small particles, there is no clay. The clay is attached to large particles, either inside or on the surface of the particles. With regard to the film obtained from the final latex (Figure 2b), it can be observed that particles are larger (than the seed) with a broad size distribution. In many polymer particles, there are aggregates of clay clearly within the polymer particles and only in a few cases on the particle surface. The number fraction of polymer particles that contain encapsulated clay is ~35%. Additional TEM images of this system are presented in the Supporting Information. Additionally, for the samples with clay contents of 0.3 and 1.7 wt %, the same trend can be observed, where the clay is encapsulated within the polymer particles (Figure 3).

Figure 4a shows the WAXD results of the films obtained from the seed and the final latex, of the blank and the sample containing 1.7 wt % clay. The unmodified Cloisite Na has a diffraction peak at 2θ = 7.4°. The diffraction angle of the

dx.doi.org/10.1021/la401301s | Langmuir 2013, 29, 9849−9856

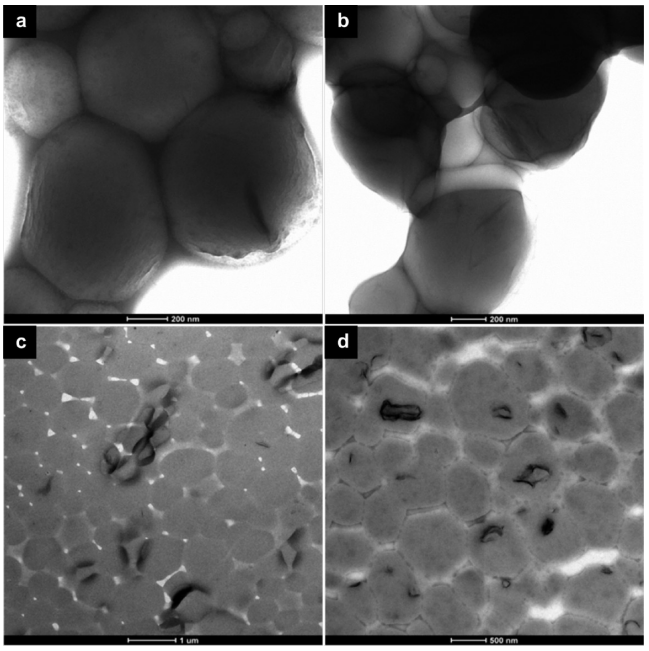

Figure 3. TEM image of the final latex for samples with (a) 0.3 and (b) 1.7 wt % clay and cross-sectional portions of the films obtained from the final latex for samples containing (c) 0.3 and (d) 1.7 wt % clay.

modified clay (2θ) decreases to 4.8°. From these data, and with the Bragg equation, it is determined that the intergallery space increases from 1.19 to 1.84 nm, because of the cationic exchange with the modifying molecules. As expected, no diffraction peaks were observed in the films without clay (seed and final latex). However, the diffraction peak of the film of the seed latex is located even at a lower diffraction angle than the modified clay (2θ = 2.7°), corresponding to an intergallery space of 3.27 nm. The same trend can be observed for samples with clay contents of 0.3 and 1.0 wt % (see the Supporting Information). This means that during the seed synthesis some growing polymer chains entered into the interlayer domains, and perhaps, some of them could react with the methacrylic group of the modifier molecule, further increasing the interlayer space. At the end of the seed preparation step, a polymer−clay intercalated structure is obtained. No peak is observed for the film of the final latex. Even if in the literature this is many times attributed to a completely exfoliated morphology, it is evident from the TEM images that although at a macroscopic level this might be the case, at the nanoscale the presence of stacks in the film is still obvious as shown in Figure 4b.

To the best of our knowledge, no clear evidence of extensive clay encapsulation has been reported before in a polymer dispersion with a high solids content (∼50 wt %). Although miniemulsion polymerization has often been used to efficiently encapsulate different inorganic fillers to obtain hybrid nanocomposites,[41,42] the encapsulation of high-aspect ratio inorganic fillers is not thermodynamically favorable; thus, the filler would preferentially remain on the surface of the monomer droplet and, therefore, of the polymer particle.[19,20] Consequently, miniemulsion polymerization by itself cannot extensively produce polymer particles with encapsulated clay. However, with this technique, it is possible to produce polymer particles that have chemically bonded clay. As clay platelets are modified with a molecule that can react during free radical polymerization, the clay may behave as a cross-linking agent, because more than one modifying molecule is on the same clay platelet. Therefore, once the clay is chemically attached either within or on the surface of the seed polymer particle, it does not move very easily during the feeding of the monomer in the second step, as a result of the high viscosity of the polymer particles.[43] Hence, once the seed particle with the nanofiller is formed by miniemulsion polymerization, the nanofiller would remain within the polymer particles after the addition of the monomer, producing encapsulation of the clay. The presence of PVA forces the latex to have colloidal particles large enough to contain clay platelets and provide good colloidal stability in the presence of clay, allowing the synthesis of dispersions with a solids content of 50 wt %, which cannot be possible with standard ionic and nonionic surfactants.[11] The main disadvantage of the proposed approach is the limited clay exfoliation, as observed in Figure 4b. The reason is that the modified clay platelets are not totally compatible with the monomer, because the edges of the clay hold hydroxyl groups that make the clay slightly hydrophilic. Furthermore, according to simulation

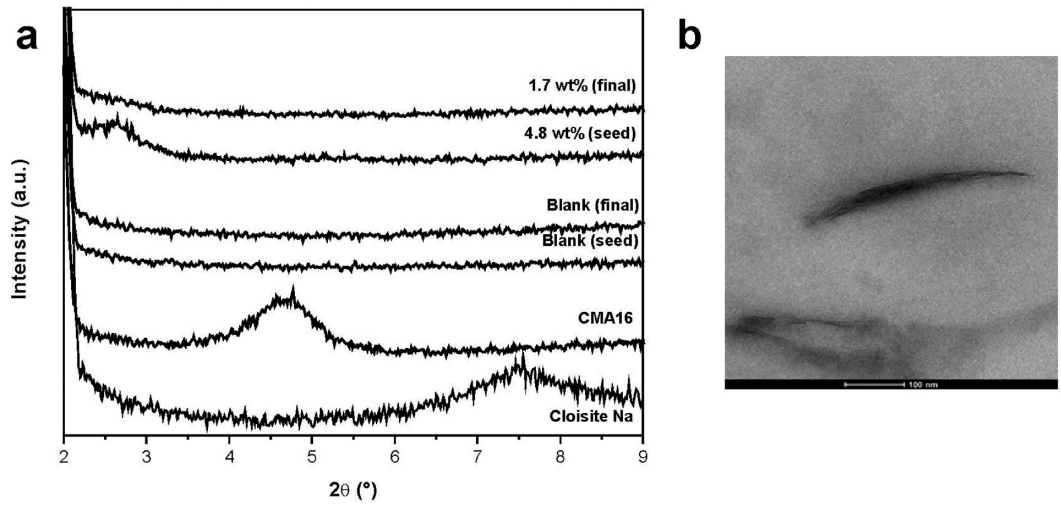

Figure 4. (a) WAXD results of the modified clay and the films from the seed and final latex of the blank and sample with a clay content of 1.7 wt %. The lines have been shifted on the *y*-axis for the sake of clarity. (b) TEM image of a clay aggregate detected in the film obtained from the final latex.

dx.doi.org/10.1021/la401301s | *Langmuir* 2013, 29, 9849−9856

results,[19,20] the clay platelets tend to aggregate, even if they were previously exfoliated, at the monomer droplet−water interface to reduce the free energy of the system.

Thermal Behavior. The DSC measurements (see the Supporting Information) reveal only one T_g at ∼36 °C for the blank sample, at an intermediate T_g value between the T_g of the PVAc (28 °C) and PVA (between 58 and 85 °C) polymers. Moreover, the obtained polymer was not fully soluble in THF, which is consistent with the grafting of PVA with PVAc that has been extensively reported for this system.[34,44,45] Although the Fox equation gives values between 32 and 36 °C (depending on the T_g used for PVA), it is worth noting that this equation is a semiempirical approximation, which is more appropriate for random copolymers than for graft (or block) copolymers. Therefore, the combination of a single T_g and a large amount of insoluble polymer suggests an extensive grafting of the PVAc with the PVA during the polymerization reaction.

One T_g was also found for the hybrid polymers. Moreover, the presence of the clay increases the T_g of the polymer ∼6 °C (see Table 2), although it is not possible to observe any trend as a function of clay content. Usually, this increment of the T_g is associated with a positive interaction of the polymer matrix with the filler, because of a shift of the dynamics of the chains close to the filler surface.[46] It has been extensively reported that the nanomaterial loading affects the T_g of the nanofiller−polymer composites. The literature is rich with examples that show an increase in T_g as clay content increases,[47] but also with works that show the opposite[46,47] and cases in which a maximal T_g is observed.[33] However, the literature emphasizes also that both the filler−polymer interfacial area and the filler−polymer matrix compatibility are responsible for the effects on T_g. For this reason, the T_g behavior in nanoclay−polymer composites, as well as the behavior of the mechanical and thermomechanical properties, is controversial because of the inherent complexity of these materials. Perhaps the lack of a clear effect with the increase in clay loading on T_g is related to the lower level of exfoliation of clay platelets,[9] and therefore a similar polymer−clay interfacial area in all the systems. The maximal decomposition temperature, $T_{d,max}$, calculated from the maximum of the derivative weight loss versus temperature curve from TGA measurements, is also given in Table 2 (the complete thermograms are shown in the Supporting Information). According to these thermograms, the thermal degradation of PVAc film and nanocomposites shows more than one degradation process. The first weight loss takes place at 50−200 °C because of the loss of adsorbed moisture and/or evaporation of the trapped water. The majority of the mass loss took place between 200 and 375 °C, which is consistent with the acetate group elimination of polymer side chains. The last step, between 400 and 550 °C, is more complex and includes the breakdown of the polymer backbone leading to the evolution of aromatic compounds.[48] The thermal decomposition behavior of the samples containing clay also passes through three steps when the samples are heated from 25 to 800 °C. There is nearly no difference in thermal decomposition behavior between pure PVAc and the PVAc−clay samples, indicating that the incorporation of clay did not substantially affect the thermal stability of the polymeric matrix. Nevertheless, in the last step, a delay in the decomposition process can be observed for the samples containing clay.

Table 2. Thermal Properties for the Samples Prepared in This Work

clay content (wt %)	T_g (°C) (DSC)	$T_{d,max}$ (°C) (TGA)
blank	36.5	323.9
0.3	42.4	321.5
1.0	41.7	321.2
1.7	42.8	323.2

Water Uptake and Rheological Properties. The water sorption curves for the blank and the nanocomposite films are

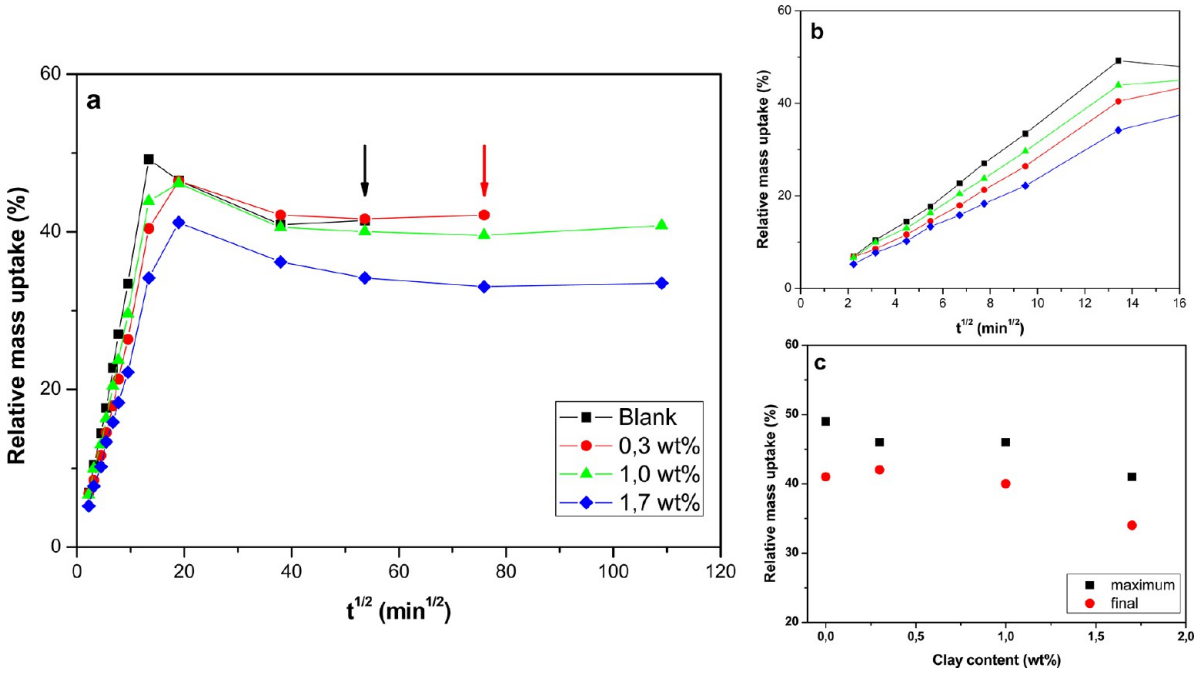

Figure 5. (a) Relative water uptake, (b) initial water uptake, and (c) maximal and saturation water uptake values of the films obtained from the final latexes prepared in this work. Arrows show the time at which specimens were broken during the experiment.

dx.doi.org/10.1021/la401301s | Langmuir 2013, 29, 9849−9856

plotted in Figure 5a. All the samples presented water sorption curves with an initial linear behavior before reaching a maximum, followed by a smooth leveling of the sorption curve to a saturation level with a longer immersion time. A first remark is that the samples without clay and with 0.3 wt % clay were difficult to handle after being immersed for 6 h in water, and they became soft and broke after immersion for 48 and 96 h, respectively (see the arrows in Figure 5a). Moreover, samples with higher clay contents were harder and could be manipulated without problems during the experiment, which can be observed in the pictures of Figure 6. The initial slope of

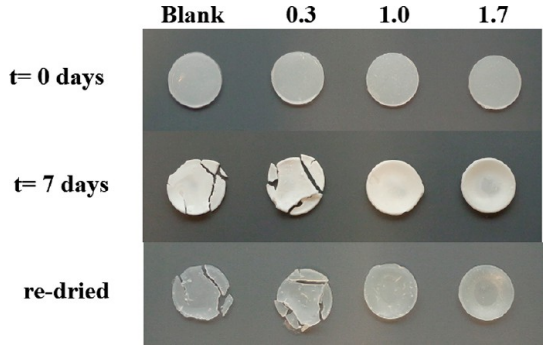

Figure 6. Pictures of water sorption specimens at 0 and 7 days and redried specimens after water immersion for the blank and nanocomposite samples.

the sorption of the blank specimen (Figure 5b) is larger than that of the specimens that contain clay, and it decreases as the clay content increases. Indeed, samples containing clay exhibit a maximal peak at longer immersion times than the blank sample. After that, a decrease in the relative level of mass uptake was observed probably because of the dissolution of salts and nongrafted PVA from the polymer film to the water bath. The maximal level of mass uptake and the maximal saturation level are plotted in Figure 5c. The trend is a slight decrease in both values with an increasing clay content. It can be noted that the clay has an effect on water uptake. It seems that the encapsulated nanostructure tends to hinder water absorption. A possible explanation can be proposed on the basis of the work of Fauchet and co-workers.[46] If the clay is encapsulated within the particles, it cannot form paths through the film that favor the access of water. As a consequence, the exudation of salts and the surfactant from the samples is likely occurring slowly. Additionally, a slight decrease in the kinetics of water sorption of the nanocomposites related to the unfilled matrix is probably due to a barrier effect associated with the large platy nanoclay particles that physically blocked the penetration of water molecules.

Figure 7 shows the storage modulus, G', and tan(δ) as a function of temperature. It can be seen above 60 °C [above the T_g (≈36 °C) of the polymer] that the value of the storage modulus in the rubbery plateau (T > 90 °C) remains unchanged for the lower-clay content sample (0.3 wt %) and is enhanced with the incorporation of the clay for the samples with higher clay contents (1.0 and 1.7 wt %). This behavior could be attributed to the restriction on the polymer chain mobility caused by the polymer−clay interactions. The tan(δ) curves showed the presence of a peak around 80 °C for the unfilled polymer, which can be attributed to the glass transition of the PVA.[49] This transition was not observed by DSC probably because of the higher heating rate and the low free

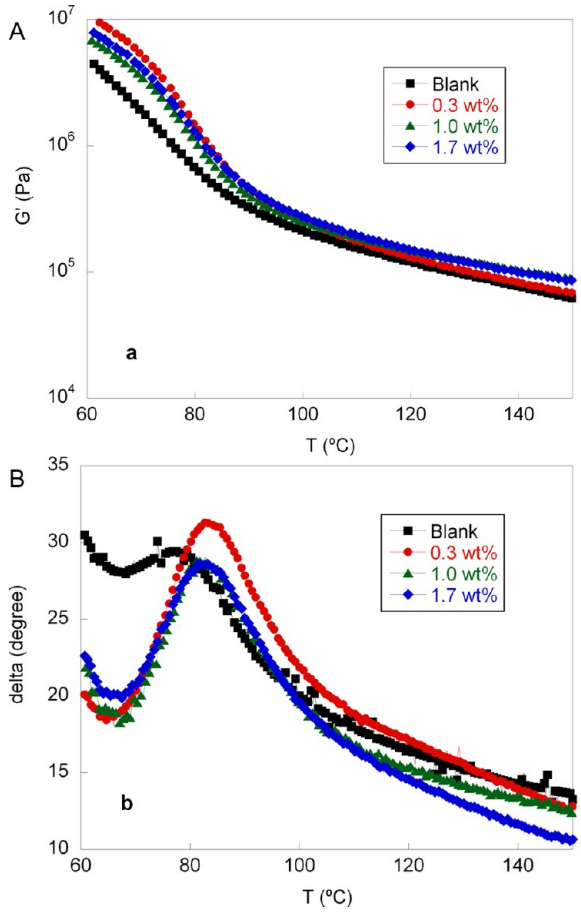

Figure 7. Effect of clay content on (a) storage modulus curves and (b) tan(δ).

PVA/grafted PVAc−PVA ratio present in the samples. The tan(δ) curves of the nanocomposite samples revealed that this transition is slightly shifted to higher temperatures with the incorporation of the clay into the polymeric matrix, regardless of clay content. This observation confirms the presence of a positive interaction of the polymeric chains with the incorporated filler.

Although Faucheu et al.[46] have found that the MMA−BA composite latex with encapsulated clays exhibits weaker mechanical improvement and a higher level of water absorption compared to those of armored clays, it should be noted that to obtain "clay-armored polymer particles" and "encapsulated clay polymer particles" a different organo-modification was employed. Therefore, in addition to the morphology, the different interactions between the clay and polymer and the effect of the organo-modifier should be taken into account in discussing the properties.

In our films, the DSC and thermomechanical results indicated the presence of a positive interaction between the clay and the polymer matrix. In addition, an improvement in the mechanical properties and water resistance of the materials demonstrated that the encapsulation of clay is relevant for obtaining materials with improved properties. Indeed, the fact that an increase in the amount of clay in the hybrid material did not decrease the values is by itself proof that a positive effect is achieved. From the industrial perspective, this means that the cost of the material can be reduced because the modified clay is cheaper than the pure polymer.

dx.doi.org/10.1021/la401301s | *Langmuir* 2013, 29, 9849−9856

CONCLUSION

In summary, this contribution reports an innovative route to the production of polymer latexes with percentages of encapsulated clay platelets in the range of 35% at industrially relevant high solids contents (50 wt %). Miniemulsion polymerization is used for the preparation of a hybrid seed. It is true, however, that miniemulsion polymerization has not yet been established as a method of choice for industry because of the additional miniemulsification step required in the plant. However, recent works have demonstrated that the use of static mixers coupled with homogenization devices or even using only static mixers in a loop configuration allows the production of miniemulsions in amounts that will meet the needs of industrial reactors. Furthermore, miniemulsion polymerization has demonstrated the ability to synthesize products that cannot be produced by means of any other polymerization in dispersed media (including the conventional and widely used emulsion polymerization) like those presented in this work.

The results of the characterization of the waterborne PVAc–clay nanocomposites showed that the incorporation of the nanoclay, using the approach described in this paper, leads to the production of polymeric materials with enhanced properties, such as higher water resistance and improved dynamical mechanical properties, compared with those of the unfilled polymer. The approach presented here might be useful for encapsulating other high-aspect ratio nanofillers, such as carbon nanotubes, graphene sheets, nonspherical nanoparticles, etc., within polymeric colloids.

ASSOCIATED CONTENT

Supporting Information

Detailed description of the characterization of the organically modified clay, additional TEM images of individual hybrid latex particles and latex films, and WAXD, DSC, and TGA measurements. This material is available free of charge via the Internet at http://pubs.acs.org.

AUTHOR INFORMATION

Corresponding Author

*E-mail: jrleiza@ehu.es (J.R.L.) and maria.paulis@ehu.es (M.P.).

Notes

The authors declare no competing financial interest.

ACKNOWLEDGMENTS

We acknowledge the funding by the University of the Basque Country UPV/EHU (UFI11/56), the Basque Government (GV IT373-10), the Ministerio de Ciencia e Innovación (MICINN, reference CTQ2011-25572), and the European Union (Woodlife Project FP7-NMP-2009-SMALL-246434). The sGIKer UPV/EHU for the electron microscopy facilities of the Gipuzkoa unit and SGI/IZO-sGIker UPV/EHU is also gratefully acknowledged. Y.R. thanks Sh. Hamzehlou for helpful suggestions and discussions. P.J.P. is member of CONICET.

REFERENCES

(1) Ray, S. S.; Okamoto, M. Polymer/Layered Silicate Nanocomposites: A Review from Preparation to Processing. *Prog. Polym. Sci.* **2003**, *28*, 1539–1641.

(2) Gao, F. Clay/Polymer Composites: The Story. *Mater. Today* **2004**, *7*, 50–55.

(3) Xu, Y.; Brittain, W. J.; Vaia, R. A.; Price, G. Improving the Physical Properties of PEA/PMMA Blends by the Uniform Dispersion of Clay Platelets. *Polymer* **2006**, *47*, 4564–4570.

(4) Pack, S.; Si, M.; Koo, J.; Sokolov, J. C.; Koga, T.; Kashiwagi, T.; Rafailovich, M. H. Mode-of-Action of Self-Extinguishing Polymer Blends Containing Organoclays. *Polym. Degrad. Stab.* **2009**, *94*, 306–326.

(5) Wang, T.; Colver, P. J.; Bon, S. A. F.; Keddie, J. L. Synergistic Effects between Clay and a Soft Polymer in a Supracolloidal Structure Leading to Increased Tack Energy in Pressure-Sensitive Adhesives. *Soft Matter* **2009**, *5*, 3842–3849.

(6) Priolo, M. A.; Gamboa, D.; Grunlan, J. C. Transparent Clay–Polymer Nano Brick Wall Assemblies with Tailorable Oxygen Barrier. *ACS Appl. Mater. Interfaces* **2010**, *2*, 312–320.

(7) Hamzehlou, Sh.; Katbab, A. A. Bottle-to-Bottle Recycling of PET Via Nanostructure Formation by Melt Intercalation in Twin Screw Compounder: Improved Thermal, Barrier, and Microbiological Properties. *J. Appl. Polym. Sci.* **2007**, *106*, 1375–1382.

(8) Wang, M.-C.; Lin, J.-J.; Tseng, H.-J.; Hsu, S. Characterization, Antimicrobial Activities, and Biocompatibility of Organically Modified Clays and Their Nanocomposites with Polyurethane. *ACS Appl. Mater. Interfaces* **2012**, *4*, 338–350.

(9) Diaconu, G.; Micusik, M.; Bonnefond, A.; Paulis, M.; Leiza, J. R. Macroinitiator and Macromonomer Modified Montmorillonite for the Synthesis of Acrylic/MMT Nanocomposite Latexes. *Macromolecules* **2009**, *42*, 3316–3325.

(10) Bourgeat-Lami, E.; Lansalot, M. Organic/Inorganic Composite Latexes: The Marriage of Emulsion Polymerization and Inorganic Chemistry. *Adv. Polym. Sci.* **2010**, *233*, 53–123.

(11) Bonnefond, A.; Paulis, M.; Leiza, J. R. Kinetics of the Emulsion Copolymerization of MMA/BA in the Presence of Sodium Montmorillonite. *Appl. Clay Sci.* **2011**, *51*, 110–116.

(12) van Herk, A. M. Historical Overview of (Mini)Emulsion Polymerizations and Preparation of Hybrid Latex Particles. *Adv. Polym. Sci.* **2010**, *233*, 1–18.

(13) Asua, J. M. Miniemulsion Polymerization. *Prog. Polym. Sci.* **2002**, *27*, 1283–1346.

(14) Goikoetxea, M.; Reyes, Y.; de las Heras, C. M.; Minari, R. J.; Beristain, I.; Paulis, M.; Barandiaran, M. J.; Keddie, J. L.; Asua, J. M. Transformation of Waterborne Hybrid Polymer Particles into Films: Morphology Development and Modeling. *Polymer* **2012**, *53*, 1098–1108.

(15) Reyes, Y.; Lopez, A.; Asua, J. M. Modeling the Microstructure of Acrylic-Polyurethane Hybrid Polymers Synthesized by Miniemulsion Polymerization. *Macromol. React. Eng.* **2011**, *5*, 352–360.

(16) Hu, J.; Chen, M.; Wu, L. Organic-Inorganic Nanocomposites Synthesized via Miniemulsion Polymerization. *Polym. Chem.* **2011**, *2*, 760–772.

(17) Micusik, M.; Reyes, Y.; Paulis, M.; Leiza, J. R. Polymer/Clay Nanocomposites by Miniemulsion Polymerization. In *Polymer Nanocomposites by Emulsion and Suspension Polymerization*; Mittal, V., Ed.; Royal Society of Chemistry: Cambridge, U.K., 2010; Chapter 10, pp 192–222.

(18) Paulis, M.; Leiza, J. R. Polymer/clay Nanocomposites through Emulsion and Suspension Polymerization. In *Advances in Polymer Nanocomposites Technology*; Mittal, V., Ed.; Nova Science Publishers: Hauppauge NY, 2009; Chapter 3, pp 53–100.

(19) Reyes, Y.; Paulis, M.; Leiza, J. R. Modeling the Equilibrium Morphology of Nanodroplets in the Presence of Nanofillers. *J. Colloid Interface Sci.* **2010**, *352*, 359–365.

(20) Micusik, M.; Bonnefond, A.; Reyes, Y.; Bogner, A.; Chazeau, L.; Plummer, C.; Paulis, M.; Leiza, J. R. Morphology of Polymer/Clay Latex Particles Synthesized by Miniemulsion Polymerization: Modeling and Experimental Results. *Macromol. React. Eng.* **2010**, *4*, 432–444.

(21) Bonnefond, A.; Micusik, M.; Paulis, M.; Leiza, J. R.; Teixeira, R. F. A.; Bon, S. A. F. Morphology and Properties of Waterborne Adhesives made from Hybrid Polyacrylic/Montmorillonite Clay Colloidal Dispersions Showing Improved Tack and Shear Resistance. *Colloid Polym. Sci.* **2013**, *291*, 167–180.

(22) Negrete-Herrera, N.; Letoffe, J.-M.; Putaux, J.-L.; David, L.; Bourgeat-Lami, E. Aqueous Dispersions of Silane-Functionalized Laponite Clay Platelets. A First Step toward the Elaboration of Water-Based Polymer/Clay Nanocomposites. *Langmuir* **2004**, *20*, 1564−1571.
(23) Voorn, D. J.; Ming, W.; van Herk, A. M. Clay Platelets Encapsulated Inside Latex Particles. *Macromolecules* **2006**, *39*, 4654−4656.
(24) Voorn, D. J.; Ming, M.; van Herk, A. M. Encapsulation of Platelets by Physical and Chemical Approaches. *Macromol. Symp.* **2006**, *245*−*246*, 584−590.
(25) Mballa Mballa, M. A.; Heuts, J. P. A.; van Herk, A. M. Encapsulation of Non-Chemically Modified Montmorillonite Clay Platelets via Emulsion Polymerization. *Colloid Polym. Sci.* **2013**, *291*, 501−513.
(26) Mballa Mballa, M. A.; Heuts, J. P. A.; van Herk, A. M. The Effect of Clay on Morphology of Multiphase Latex Particles. *Colloid Polym. Sci.* **2013**, *291*, 1419−1427.
(27) Diaconu, G.; Paulis, M.; Leiza, J. R. Towards the Synthesis of High Solids Content Waterborne Poly(methyl methacrylate-co-butyl acrylate)/Montmorillonite Nanocomposites. *Polymer* **2008**, *49*, 2444−2454.
(28) Lim, T. L.; Park, O. O. Phase Morphology and Rheological Behavior of Polymer/Layered Silicate Nanocomposites. *Rheol. Acta* **2001**, *40*, 220−229.
(29) Faucheu, J.; Gauthier, C.; Chazeau, L.; Cavaillé, J.-Y.; Mellon, V.; Bourgeat Lami, E. Miniemulsion Polymerization for Synthesis of Structured Clay/Polymer Nanocomposites: Short Review and Recent Advances. *Polymer* **2010**, *51*, 6−17.
(30) Fornes, T. D.; Paul, D. R. Modeling Properties of Nylon 6/Clay Nanocomposites Using Composite Theories. *Polymer* **2003**, *44*, 4993−5013.
(31) Zeng, C.; Lee, L. J. Poly(methyl methacrylate) and Polystyrene/Clay Nanocomposites Prepared by in-Situ Polymerization. *Macromolecules* **2001**, *34*, 4098−4113.
(32) Ruzicka, B.; Zaccarelli, E.; Zulian, L.; Angelini, R.; Sztuck, M.; Moussaïd, A.; Narayanan, T.; Sciortino, F. Observation of Empty Liquids and Equilibrium Gels in a Colloidal Clay. *Nat. Mater.* **2011**, *10*, 56−60.
(33) García-Chávez, K. I.; Hernández-Escobar, C. A.; Flores-Gallardo, S. G.; Soriano-Corral, F.; Saucedo-Salazar, E.; Zaragoza-Contreras, E. A. Morphology and Thermal Properties of Clay/PMMA Nanocomposites Obtained by Miniemulsion Polymerization. *Micron* **2013**, *49*, 21−27.
(34) Bohorquez, S. J.; Asua, J. M. Particle Nucleation in High Solids Batch Miniemulsion Polymerization Stabilized with a Polymeric Surfactant. *J. Polym. Sci., Part A: Polym. Chem.* **2008**, *46*, 6407−6415.
(35) Linares, E. M.; Rippel, M. M.; Galambeck, F. Clay Platelet Partition within Polymer Blend Nanocomposite Films by EFTEM. *ACS Appl. Mater. Interfaces* **2010**, *2*, 3648−3653.
(36) Etmimi, H. M.; Sanderson, R. D. New Approach to the Synthesis of Exfoliated Polymer/Graphite Nanocomposites by Miniemulsion Polymerization Using Functionalized Graphene. *Macromolecules* **2011**, *44*, 8504−8515.
(37) Ruggerone, R.; Plummer, C.; Negrete-Herrera, N.; Bourgeat-Lami, E.; Manson, J.-A. Highly Filled Polystyrene−Laponite Nanocomposites Prepared by Emulsion Polymerization. *Eur. Polym. J.* **2009**, *45*, 621−629.
(38) Keddie, J. L.; Routh, A. F. *Fundamentals of Latex Film Formation; Processes and Properties*; Springer: Dordrecht, The Netherlands, 2010.
(39) Bandrup, J.; Immergut, E. H.; Grulke, E. A. *Polymer Handbook*; Wiley-Interscience: New York, 2003.
(40) Finch, C. A. *Polyvinyl alcohol developments*; John Wiley & Sons: West Sussex, U.K., 1992.
(41) Landfester, K. Miniemulsion Polymerization and the Structure of Polymer and Hybrid Nanoparticles. *Angew. Chem., Int. Ed.* **2009**, *48*, 4488−4507.
(42) Aguirre, M.; Paulis, M.; Leiza, J. R. UV Screening Clear Coats Based on Encapsulated CeO_2 Hybrid Latexes. *J. Mater. Chem. A* **2013**, *1*, 3155−3162.
(43) Durant, Y. G.; Sundberg, E. J.; Sundberg, D. C. Effects of Cross-Linking on the Morphology of Structured Latex Particles. 2. Experimental Evidence for Lightly Cross-Linked Systems. *Macromolecules* **1997**, *30*, 1028−1032.
(44) Suzuki, A.; Yano, M.; Saiga, T. Study on the Initial Stage of Emulsion Polymerization of Vinyl Acetate Using Poly(Vinyl Alcohol) as a Protective Colloid. *Colloid Polym. Sci.* **2003**, *281*, 337−342.
(45) Budhlall, B. M.; et al. Role of Grafting in the Emulsion Polymerization of Vinyl Acetate with Poly(vinyl alcohol) as an Emulsifier. I. Effect of the Degree of Blockiness on the Kinetics and Mechanism of Grafting. *J. Polym. Sci., Polym. Chem.* **2001**, *39*, 3633−3654.
(46) Faucheu, J.; Gauthier, C.; Chazeau, L.; Cavaillé, J.-Y.; Mellon, V.; Pardal, F.; Bourgeat Lami, E. Properties of Polymer/Clay Interphase in Nanoparticles Synthesized Through in-Situ Polymerization Processes. *Polymer* **2010**, *51*, 4462−4471.
(47) Zengeni, E.; Hartmann, P.; Pasch, H. Encapsulation of Clay by Ad-Miniemulsion Polymerization: The Influence of Clay Size and Modifier Reactivity on Latex Morphology and Physical Properties. *ACS Appl. Mater. Interfaces* **2012**, *4*, 6957−6968.
(48) Holland, B. J.; Hay, J. N. The Thermal Degradation of Poly(Vinyl Acetate) Measured by Thermal Analysis−Fourier Transform Infrared Spectroscopy. *Polymer* **2002**, *43*, 2207−2211.
(49) López-Suevos, F.; Eyholzer, C.; Bordeanu, N.; Richter, K. DMA Analysis and Wood Bonding of PVAc Latex Reinforced with Cellulose Nanofibrils. *Cellulose* **2010**, *17*, 387−398.